

# Evaluating the Roles of Thrombin and Calcium in the Activation of Coagulation Factor XIII Using H/D Exchange and MALDI-TOF MS<sup>†</sup>

Brian T. Turner, Jr. and Muriel C. Maurer\*

Department of Chemistry, University of Louisville, Louisville, Kentucky 40292

Received February 4, 2002; Revised Manuscript Received April 4, 2002

**ABSTRACT:** Factor XIII catalyzes the formation of isopeptide bonds between noncovalently associated fibrin monomers in the final stages of the blood coagulation cascade. This results in a rigid, covalently linked network that is much more resistant to proteolytic degradation. Calcium ion is critical to this process, and its continued presence after activation aids in maintenance of Factor XIII activity. Hydrogen/deuterium exchange experiments were conducted on recombinant Factor XIII  $a_2$  using matrix-assisted laser desorption ionization time-of-flight mass spectrometry. The method revealed changes in the structure of Factor XIII  $a_2$  localized to different areas of the protein that were related to the manner in which the enzyme was activated and the calcium environment in which it was maintained. A possible substrate recognition region in the catalytic core (220–230) shows an increase in deuteration upon activation. The degree of deuteration varies depending on the calcium environment in which the active enzyme is maintained. A portion of the  $\beta$ -sandwich domain (98–104) exhibits a decrease in deuteration upon activation by exposure to calcium alone. A third change occurs in the  $\beta$ -barrel 1 domain of the protein, a portion of which (526–546) shows a decrease in deuteration upon activation by calcium exposure, but almost none at all when the enzyme is activated by thrombin. The pattern of observed changes reveals individual contributions of calcium and thrombin to activating the enzyme toward substrate binding and exposure of the active site.

The blood coagulation cascade is a complex and tightly regulated sequence of biochemical reactions. The events of the latter portion of the cascade have been well studied, but are not as well understood with regards to substrate specificity and reactivity. In these final steps, the serine protease thrombin cleaves the *N*-terminal fragments from the  $\alpha$  and  $\beta$  chains of the large structural protein fibrinogen ( $\alpha\alpha\beta\beta$ )<sub>2</sub>, exposing sites that allow fibrin monomers to aggregate linearly and laterally. The resultant loose, noncovalently associated network is converted into a covalently cross-linked mesh through the action of Factor XIII (FXIII).<sup>1</sup> This coagulation enzyme catalyzes the formation of isopeptide bonds between certain glutamine and lysine side chains located in the  $\alpha$  and  $\gamma$  chains of fibrin (reviewed in 1). The cross-linking action of FXIII also serves to incorporate other proteins, such as  $\alpha_2$ -antiplasmin, into the fibrin network (2).

Factor XIII is a 731-amino acid transglutaminase occurring naturally in two forms. The plasma form circulates within the bloodstream as a tetramer composed of two a-subunits and two b-subunits ( $a_2b_2$ ), of approximately 83 and 80 kDa

each, respectively. The second form is found in platelets and placenta and consists solely of the  $a_2$  dimer. The catalytic machinery of the enzyme is contained within the a-subunit. The b-subunit is proposed to play a regulatory role, or perhaps act as a carrier for the a-subunits, and dissociates from the a-subunit upon activation of plasma FXIII. Recombinant human placental FXIII (rFXIII), containing only the  $a_2$  dimer and overexpressed in *Saccharomyces cerevisiae* (3), was used in the current study.

The FXIII a-subunit consists of five distinct structural domains (Figure 1). A 37-residue *N*-terminal activation peptide is cleaved upon thrombin activation of the enzyme. The  $\beta$ -sandwich domain spans residues 38–183. The catalytic core is comprised of residues 184–515. The  $\beta$ -barrel 1 and  $\beta$ -barrel 2 are composed of residues 516–627 and residues 628–731, respectively. The enzyme contains a catalytic triad very similar to that of a cysteine protease in the catalytic core domain, consisting of Cys314, His373, and Asp396 (reviewed in 4). The transglutaminase mechanism is proposed to be the reverse of the proteolysis mechanism for cysteine proteases (5).

Thrombin activates FXIII by hydrolyzing the activation peptide between residues 37–38. Calcium is also critical to the activation of FXIII. A putative calcium-binding site has been located by X-ray crystallography that consists of Asp438, Glu485, and Glu490 (6). It is also known that thrombin-cleaved rFXIII in the absence of calcium is less active than the same enzyme in the presence of calcium (7). Previous studies have shown that zymogenic rFXIII can attain activity in the presence of high, nonphysiological concentrations of calcium alone (>50 mM), or at low

<sup>†</sup> This work was supported by a University of Louisville Research Initiation Grant.

\* Corresponding author. Tel: (502) 852-7008. Fax: (502) 852-8149. E-mail: muriel.maurer@louisville.edu.

<sup>1</sup> Abbreviations: rFXIII, recombinant human placental factor XIII; MALDI-TOF MS, matrix-assisted laser desorption/ionization time-of-flight mass spectrometry;  $a_2$ , zymogen form of rFXIII;  $a_2'$ , rFXIII activated by thrombin cleavage in the presence of calcium and resuspended in a calcium-free buffer;  $a_2^*$ , rFXIII activated by thrombin cleavage in the presence of calcium and resuspended in a buffer containing 1 mM CaCl<sub>2</sub>;  $a_2^{*Ca}$ , rFXIII activated nonproteolytically by exposure to 50 mM CaCl<sub>2</sub> and resuspended in a buffer containing 1 mM CaCl<sub>2</sub>; CAPP, Centroid Application software.

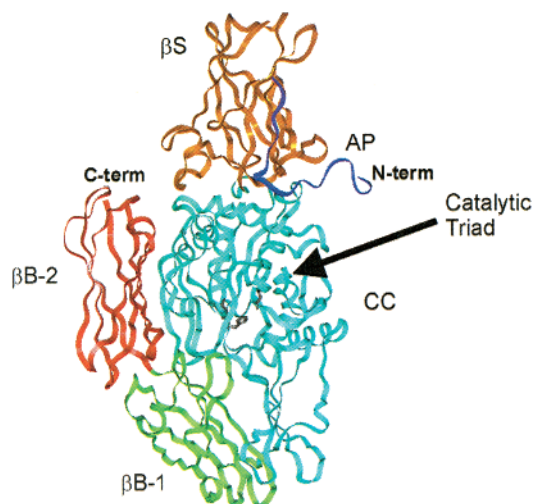


FIGURE 1: Domain structure of Coagulation Factor XIII, single a-subunit. Ribbon diagram from the X-ray crystal structure 1FIE (thrombin-cleaved FXIII a-subunit) (14). The figure is color-coded to highlight the five domains: activation peptide (AP, purple),  $\beta$ -sandwich ( $\beta$ S, orange), catalytic core (CC, light blue),  $\beta$ -barrel 1 ( $\beta$ B-1, green), and  $\beta$ -barrel 2 ( $\beta$ B-2, red). The residues of the catalytic triad (Cys 314, His 373, and Asp 396) are depicted as black sticks within the catalytic core domain.

calcium concentrations and high sodium chloride (8, 9). Fibrin also plays a substantial role in FXIII activation; its presence has been shown to greatly accelerate the rate of activation of FXIII (10–12).

The roles of thrombin cleavage and calcium ion in the activation of FXIII have been thoroughly investigated kinetically, but their effect remains unclear from a structural standpoint. In platelet FXIII, thrombin cleavage alone is sufficient for the generation of activity (13). This activity is enhanced by the addition of calcium. The active site residues of FXIII buried within the catalytic core of each a-subunit are thought to become more exposed upon calcium binding through a conformational change. Calcium has been proposed to act as an allosteric effector that could trigger such a conformational change in one of the two a-subunits, perhaps the one uncleaved by thrombin (7, 12).

X-ray crystallography shows that the activation peptide appears to mask the active site of the opposite a-subunit within the dimer (14). The zymogenic form of FXIII, the thrombin-cleaved activated form, and the uncleaved form in the presence of calcium have all been subjected to numerous crystallographic studies (6, 7, 14–17). However, all of these structures have proven to be quite similar to one another, and there is no evidence of a large conformational change that would expose the active site (16). It has been hypothesized that the very act of crystallizing the calcium-bound enzyme may restrict it from assuming its active conformation (17) by confining it to the unnatural constraints of a unit cell.

Crystallography has contributed much to our understanding of FXIII on a structural level; however, it provides only static “snapshots” of this complex biological molecule in one of many possible conformations. This dynamic system should be studied under solution conditions, if possible. One method that could complement and expand upon the information obtained from crystal structures involves the use of hydrogen/deuterium exchange of amide protons as a measure of the

percent deuteration of different portions of the protein. If a conformational change occurs upon activation, certain regions of the enzyme should become more exposed to the solvent and thus more susceptible to H/D exchange. Other regions may become buried and resist isotope exchange. Peptides bearing an increased or decreased number of deuterons in the activated enzyme when compared to the same sites in the inactive zymogen form would offer evidence in favor of such conformational changes.

Our current study examines the enzyme in four different forms, differing in the mode of activation of the enzyme and the calcium environment in which it is maintained: (1) the zymogen form ( $a_2$ ), to which all other states are referenced, (2) the thrombin-cleaved form maintained in the absence of calcium ( $a_2'$ ), (3) the thrombin-cleaved form maintained in the presence of 1 mM calcium ( $a_2^*$ ), and (4) the enzyme nonproteolytically activated by exposure to 50 mM calcium and maintained in a 1 mM calcium buffer ( $a_2^{*Ca}$ ). Note that 12 mM  $CaCl_2$  was present in the activation medium in each of the thrombin-cleaved cases before it was either removed or reduced to lower levels.

We utilized the H/D exchange method to study the changes occurring upon the activation of FXIII by thrombin and calcium. Moreover, we have conducted our experiments in such a way as to separate the effects of thrombin cleavage from calcium binding. NMR spectroscopy has previously been used to characterize isotope exchange. NMR is of limited utility in this instance; however, where the protein being studied is extremely large, yielding many overlapping resonances that are difficult to interpret. An alternative technique for observing H/D exchange is mass spectrometry, both electrospray (18) and MALDI-TOF (19). MALDI-TOF MS is used here to characterize the extent of deuteration at each portion of the enzyme. Fragmentation of the deuterated protein using a protease such as pepsin allows the localization of changes in percent deuteration. The technique has been used to study a number of protein systems, including methylesterase CheB (20), protein kinase A (21), MAP kinase kinase I (22), SH2 domains (23), and viral coat proteins (24, 25).

Our results reveal subtle changes in the structure of rFXIII upon activation localized to different areas of the protein. These changes appear to be related to the manner in which the enzyme is activated and the calcium environment in which it is maintained. Specifically, a portion of the  $\beta$ -sandwich domain exhibits a decrease of 8.37% in deuteration upon activation by calcium exposure. A particular segment of the catalytic core shows a 4.55% increase in deuteration when activated. The degree of deuteration varies depending on the calcium environment of the active enzyme. The third significant change occurs in a portion of the  $\beta$ -barrel 1 domain, which shows a 6.83% decrease in deuteration upon activation by calcium exposure but almost none at all when the enzyme is cleaved by thrombin. The pattern of changes observed may reveal individual contributions of calcium and thrombin to the activity of the enzyme.

## EXPERIMENTAL PROCEDURES

**Protein Preparation.** Recombinant human placental Factor XIII, consisting of the  $a_2$  dimer, was generously provided by Dr. Paul Bishop of ZymoGenetics, Inc. (Seattle, WA)

(3). Stock solutions were prepared by dissolving the powdered material in deionized water. The concentration was verified by measuring the absorbance of the solution at 280 nm (extinction coefficient =  $1.49 \text{ mL mg}^{-1} \text{ cm}^{-1}$ ). The concentration of protein in the stock solution was adjusted to  $40 \mu\text{M}$  ( $3.15 \text{ mg/mL}$ ), based on the molecular weight of a single  $\alpha$ -subunit, 83 kDa.

rFXIII stock solution was activated by thrombin cleavage to the  $\alpha_2'$  or  $\alpha_2^*$  forms in a 20 mM borate buffer, pH 8.3. The activation medium contained calcium chloride (12 mM) and activated bovine thrombin (37 nM). The thrombin employed was purified from bovine citrate eluate using the method of Trumbo and Maurer (26). The activation medium was incubated at  $37^\circ\text{C}$  for 12 min. PPACK (Phe-Pro-Arg chloromethyl ketone) was then added to inhibit thrombin, and the mixture was incubated an additional 12 min at  $37^\circ\text{C}$ . FXIII activity was verified by the Berichrom coupled assay (27), using reconstituted kit components purchased from commercial vendors. Antihuman thrombin monoclonal antibody covalently bound to Protein G beads was then added to the activation medium. The mixture was incubated at room temperature for 10 min, and antibody beads were removed by centrifugation. Mass spectra of the purified FXIII show no signs of thrombin contamination. The supernatant liquid containing the activated FXIII was placed in Slide-a-Lyzer dialysis cassettes (Pierce) with a 10 kDa molecular weight cutoff (MWCO) and dialyzed for 3 h at  $4^\circ\text{C}$  against 6.67 mM borate buffer at pH 8.3 with or without 0.33 mM  $\text{CaCl}_2$ , depending on whether it was desired to retain calcium. Buffer exchange was achieved in some experiments by loading the material into Centricon-50 concentrator tubes (Amicon, Beverly, MA) of 50 kDa MWCO, adding excess buffer, and centrifuging until the desired concentration of protein was reached. The dialysate was divided into aliquots of  $36 \mu\text{L}$  each and evaporated to dryness using a SpeedVac concentrator (Savant).

Alternatively, rFXIII was left in the zymogen form  $\alpha_2$  or activated nonproteolytically to the  $\alpha_2^{*\text{Ca}}$  state. In this activation procedure, rFXIII stock solution was combined with equal quantities of 20 mM borate buffer at pH 8.3 and 150 mM  $\text{CaCl}_2$  solution (final calcium concentration = 50 mM). The mixture was incubated at  $37^\circ\text{C}$  for 2 h. The Berichrom assay shows the material has an activity equal to that of rFXIII  $\alpha_2^*$ . The material was exchanged into a buffer containing 6.67 mM boric acid and 0.33 mM  $\text{CaCl}_2$  and dehydrated as described above.

**Hydrogen/Deuterium Exchange Experiments.** Dry protein aliquots were reconstituted in  $12 \mu\text{L}$  of 99.996%  $\text{D}_2\text{O}$  (Cambridge Isotope Laboratories) to produce a  $40 \mu\text{M}$  solution of FXIII in a 20 mM borate buffer (with or without 1 mM  $\text{CaCl}_2$ ). These solutions were allowed to incubate at room temperature for 1, 2, or 5 min. Following the prescribed incubation period, the H/D exchange was rapidly quenched by 11-fold dilution in chilled 0.1% trifluoroacetic acid (TFA) at pH 2.5. A small amount of 2% TFA was also added to ensure that the solution pH was 2.5. This amount was determined by tests conducted on nondeuterated protein solutions. The quenched solution was added to immobilized pepsin gel (pepsin covalently bound to 6% agarose, Pierce Chemical) and incubated on ice for 10 min. Pepsin was removed by centrifugation at  $4^\circ\text{C}$ . Ten microliter aliquots

of the supernatant liquid were withdrawn, placed in plastic microfuge tubes, and immediately immersed in liquid nitrogen. Samples were stored at  $-70^\circ\text{C}$  until analysis. Each H/D exchange timepoint experiment was performed in triplicate.

**Analysis of Peptic Digests by MALDI-TOF Mass Spectrometry.** Frozen samples were rapidly defrosted and mixed with equal volume of chilled matrix solution ( $\alpha$ -cyano-hydroxycinnamic acid [Aldrich], 5 mg/mL in 1:1:1 ethanol/acetonitrile/0.1% TFA, pH 2.2). One microliter of the mixture was spotted to a pre-chilled stainless steel MALDI plate. Sample spots were dried under moderate vacuum for no more than 90 s in the SpeedVac device. The plate was immediately transferred to the Voyager DE-Pro mass spectrometer (Applied Biosystems, Forest City, CA). A spectrum was acquired within 5 min of defrosting the sample. Spectra were acquired in reflector mode over a mass range of 800–3000  $m/z$  with 256 laser shots per spectrum.

**Peptide Identification.** Approximately 50 peptides are observed in peptic digests of rFXIII, spanning the mass range 800–3000  $m/z$ . A number of the peptides were identified by a combination of accurate mass matching and MALDI-TOF post source decay (PSD). Other peptides were identified by C-terminal ladder sequencing using Carboxypeptidase-Y (28). Peak masses from the mass spectrum of a peptic digest of undeuterated FXIII were calibrated against peptides of known molecular mass. Monoisotopic masses were then submitted to the program GPMW (General Protein/Mass Analysis for Windows—Lighthouse Data, Denmark) for matching to all possible continuous sequences derived from the human Factor XIII  $\alpha$ -chain. Best results for PSD and CPY ladder sequencing were obtained when the peptic digest was separated into fractions containing no more than three peptides each using high-performance liquid chromatography on a  $3.9 \times 150 \text{ mm}$  NovaPak C18 column (Waters). Elution was performed using a water/acetonitrile gradient (5 to 50% organic over 80 min), each containing 0.09% TFA.

**Data Analysis.** Spectra were calibrated in a two-point procedure using GRAMS 386 software (Galactic). Reference peptides selected for calibration had molecular weights of 849.4708 and 1215.6975 Da (singly protonated monoisotopic masses 850.4787 and 1216.7054 Da, respectively). These peptides had been previously identified by post-source decay analysis. Deuterium content of each peptide present in the digest was determined by integration of the isotopic envelope using CAPP (Centroid APPLICATION) for Windows (Dr. J. G. Mandell, UCSD) (19). The centroids of peptides derived from a digest of undeuterated FXIII were then subtracted from these numbers to obtain the number of deuterons present in each peptide at a particular time point. The data were then fitted to a two-parameter exponential equation of the form  $D = a(1 - e^{-bt})$  using SigmaPlot, in which  $D$  represents the average number of deuterons incorporated by a peptide at time  $t$ . The  $a$  parameter represents the maximum amount of deuterium uptake by a peptide over a 5-minute period. The parameter  $b$  serves as a rate constant for isotope exchange within this particular peptide. Due to the small number of data points used for the fitting, the  $b$  value obtained is believed to be unreliable as a measure of the rate of isotope exchange. The fitting is performed primarily to obtain the value of  $a$ .



1 SETSRTAFGG RRAVPPNNNS AAEDDLPTVE LQGVVPRGVN LQEFNLVTSV 50  
 51 HLFKERWDTN KVDHHTDKYE NNKLIVRRGO SEYVQIDFSR PYDPRRRDLFR 100  
 101 VEYVIGRYFQ ENKGTYPVP IVSELOSGKW GAKIVMREDR SVRLSIQSSP 150  
 151 KCIVGKFRMY VAVWTPYGV LRTSRNPETDT YILFNPCWED DAVYLDNEKE 200  
 201 REEYVLNDIG VIFYGEVNDI KTRSWYSGQF EDGILDTCLY VMDRAQMDLS 250  
 251 GRGNPIKVS R VGSAMVNAKD DEGVLVGSWD NIYAYGVPPS AWTGSVDIIL 300  
 301 EYRSSENPRV YGQCWFAGV FNTFLRCLGI PARIVTNYFS AHDNDANLQM 350  
 351 DIFLEEDGNV NSKLTKDSVM NYHCWNEAWM TREDLEPVGFG GWQAVDSTPG 400  
 401 ENSDGMRYCG PASVQAIRHG HVCFQFDAPF VFAEVNSDLI YITAKKDGTH 450  
 451 VVENVDATHI GKLIVTKQIG GDGMMDITDT YKFQEGQEEE RLALETALMY 500  
 501 GAKKPLNTEG VMKSRSNVDM DFEVENAVLG KDFKLSITFR NNSHNRYTIT 550  
 551 AYL SANITFY TGVPKAEFKK ETFDVTLEPL SFKKEAVLIQ AGEYMGQLLE 600  
 601 QASLHFFVTA RINETRDVLA KQKSTVLTP EIIIKVRGTQ VVGSMDMTVT 650  
 651 QFTNPLKETL RNWVHLDDG GVTRPMKKMF REIRPNSTVQ WEEVCRPWVS 700  
 701 GHRKLIASMS SDSLRHVYGE LDVQIQRPS M 731

FIGURE 2: Sequence coverage of the rFXIII a-subunit by peptic digest. Peptides identified are represented by solid and dashed underlined sequences. The coverage is 45.5% of the a-subunit's sequence. The peptides considered most suitable for obtaining H/D exchange data cover approximately 29% of the total sequence and are indicated by the solid lines. Peptide sequences indicated by the dashed underlines are less suitable due to the degree of overlap of their isotopic clusters with those of other peptides either before or after deuteration.

## RESULTS

**Sequence Coverage of FXIII in Peptic Digests.** Treatment of rFXIII with pepsin results in 50 peptide fragments in the molecular weight range of 800–3000 Da that display peaks of acceptable intensity (>1000 counts on a scale of 0–64000 counts) when subjected to MALDI-TOF mass spectrometry. Pepsin is most often used in studies of this variety because it is the only commercially available protease that is most active at pH 2.5, the condition at which isotope exchange is at its minimum rate (29, 30). Pepsin cleavage of a protein is quite nonspecific, and it is difficult to predict what sites will be cleaved in advance. However, pepsin's cleavage pattern for a particular protein is reproducible.

Of the 50 product peptides, 35 have been identified using sequence matching, post-source decay sequencing and C-terminal ladder sequencing with the endopeptidase carboxypeptidase-Y. High-performance liquid chromatography was used to separate peptic digests for sequencing. The peptides identified represent 45.5% coverage of the FXIII a-chain sequence, as seen in Figure 2 (solid and dashed underlined sequences). Similar digests performed with trypsin (data not shown), a much more specific protease, have resulted in no more than 50% coverage of the protein's sequence. Of the 50 peptides observed in a typical mass spectrum, 22 nonoverlapping peptide peaks were routinely monitored for gathering H/D exchange data (solid underlined sequences only, Figure 2).

**Hydrogen/Deuterium Exchange Experiments.** rFXIII in four different states,  $a_2$ ,  $a_2'$ ,  $a_2^*$ , and  $a_2^{*Ca}$ , was subjected to periods of deuteration ranging from 1 to 5 min by dissolving the lyophilized protein in 100%  $D_2O$ . As deuterium is incorporated at the amide positions of a protein, the mass envelope of a peptide peak derived from an affected region of the protein changes appearance and shifts to higher  $m/z$ . Centroids of deuterated peptide mass envelopes measured

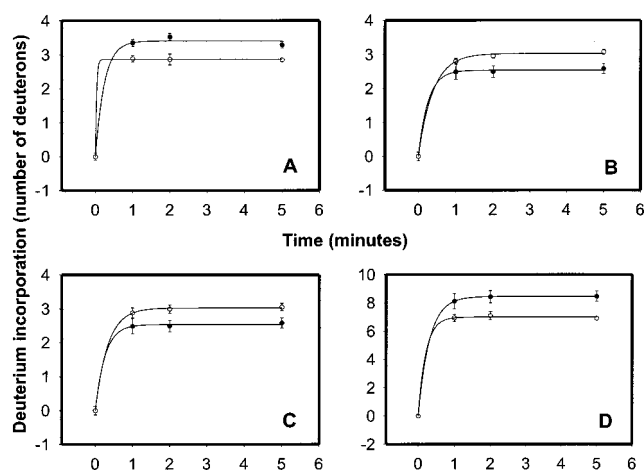


FIGURE 3: Representative deuteration profiles for peptides derived from the peptic digest of rFXIII. Deuterium incorporation of three peptic peptides derived from the Factor XIII a-subunit as a function of time. Filled circles are for the zymogen ( $a_2$ ) state of the protein. The hollow circles represent another state of the protein, as described below. Error bars for each data point are the standard deviation of the mean for three independent experiments. Data points were fit to the equation  $D = a(1 - e^{-bt})$  by SigmaPlot. Panel A: Residues 98–104, nonproteolytically activated ( $a_2^{*Ca}$ ). Panel B: Residues 220–230, thrombin-cleaved ( $a_2^*$ ). Panel C: Residues 220–230, nonproteolytically activated ( $a_2^{*Ca}$ ). Panel D: Residues 526–546, nonproteolytically activated ( $a_2^{*Ca}$ ).

relative to their nondeuterated counterparts yield the average number of deuterons the peptide has incorporated. The kinetics of deuteration for each peptide were fit to a single-exponential equation to obtain the average number of deuterons a peptide incorporated within a five minute period. Representative results are shown in Figure 3.

Note that all of the peptides under observation reached a maximum deuterium incorporation within 5 min of exposure to  $D_2O$ . Exposure to  $D_2O$  for longer times (10–15 min, data not shown) did not result in further significant deuterium incorporation. Short times were chosen to ensure that only solvent-accessible surface amide hydrogens would exchange for deuterium. Longer deuteration times may have resulted in the deuteration of protein regions not normally accessible to the solvent. Side chain protons, such as the acidic or basic protons of aspartic acid and lysine residues, also undergo exchange, although at a much more rapid rate. Almost all of the deuterium incorporated in these side chains, as well as by the N- and C-termini of the protein, is lost within seconds of quenching. Their contribution to the total deuterium content is proportional to the amount of  $D_2O$  remaining in the quenched peptide solution and is therefore minor.

Back-exchange of deuterated amides for hydrogen after quenching accounts for an approximately 40% loss of the label under normal sample handling conditions, as judged by deuteration experiments performed on small model peptides (data not shown). The back-exchange reaction is believed to occur at a constant rate, as evidenced by a low degree of variance among independent experiments. No effort has been made to correct for this loss in the results shown. If only the difference in percent deuteration between two states of a protein is desired, the deuteration profiles of the two states of the protein should be directly comparable.

**Changes in Percent Deuteration.** Three peptides display the greatest degree of change in deuteration among the three

Table 1: Changes in Percent Deuteration of Portions of Factor XIII's  $\alpha$ -Subunit

peak mass ( $m/z$ )	amino acids	theoretical max <sup>a</sup> (no. of D's)	$a_2^{*Ca}$		$a_2'$		$a_2^*$	
			D-on <sup>b</sup>	% change <sup>c</sup>	D-on	% change	D-on	% change
925.5171	98–104	6.45	−0.54	−8.37	n/a	n/a	n/a	n/a
1013.4779	240–247 <sup>d</sup>	7.54	0.28	~4	0.23	~3	0.39	~5
1198.5746	513–522	9.72	−0.20	−2.06	−0.11	−1.13	−0.24	−2.47
1372.7456	220–230	10.77	0.49	4.55	0.31	2.88	0.49	4.55
1800.9217	4–20	17.125	0.31	1.81	0.36	2.10	0.49	2.89
2431.3052	526–546	21.215	−1.45	−6.83	−0.09	−0.42	−0.76	−3.58

<sup>a</sup> Theoretical max represents the maximum number of exchangeable protons present in a particular peptide. It is composed of all the backbone amide protons plus a fraction of C- and N-terminal protons and exchangeable side chain protons dependent upon the amount of D<sub>2</sub>O present in the system under quench conditions (approximately 5%). A peptide that is “100% deuterated” would be expected to contain this number of deuterons.

<sup>b</sup> All D-on's and % changes measured relative to zymogen rFXIII ( $a_2$ ). <sup>c</sup> % change is calculated by dividing the D-on value by the theoretical max for the peptide in question and multiplying by 100%. <sup>d</sup> The D-on and % change figures for the 240–247 peptide are calculated using an overlapped peak cluster. The values themselves are approximations. The measurements here should be considered more qualitatively than quantitatively due to the degree of overlap with a previous peak cluster.

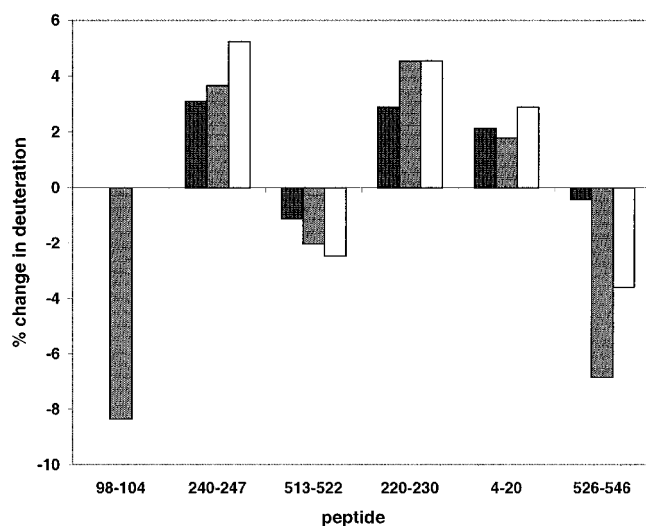


FIGURE 4: Observed changes in percent deuteration. This figure is a graphical representation of the information presented in Table 1. Black bars indicate  $a_2'$ , white bars for  $a_2^*$ , and gray bars  $a_2^{*Ca}$ .

states of the enzyme being observed. Each of these peptides experienced an increase or decrease in percent deuteration, representing at least 4.5% of the theoretical maximum number of deuterons that can be accepted. More minor, and perhaps less reliable, changes are observed, each characterized by a 2.5–3% change in deuteration per peptide.

The results are summarized in Table 1 and Figure 4. The three peptides exhibiting the most significant changes in percent deuteration are derived from distinct domains of rFXIII. All have been identified. The peak at 925.5171  $m/z$  corresponds to amino acid residues 98–104 and is localized to the  $\beta$ -sandwich domain of the enzyme. A second peak at 2431.3052  $m/z$  represents residues 526–546 of the enzyme and is from the  $\beta$ -barrel 1 domain. A third peak, 1372.7456  $m/z$ , is from the peptide spanning residues 220–230, which is located in the catalytic core of the enzyme. The percentage change shown represents the difference between the peptide centroids of a particular enzyme state and the zymogen (the value stated as “D-on” in Table 1) divided by the theoretical maximum shown in Table 1.

A noteworthy change on exposure to calcium occurs in the peptide spanning residues 526–546 in the  $\beta$ -barrel 1 domain (see also Figure 5D). The 1.37 Da decrease in the centroid of this peptide due to calcium exposure ( $a_2^{*Ca}$ ) represents a net decrease in degree of deuteration of 6.8%.

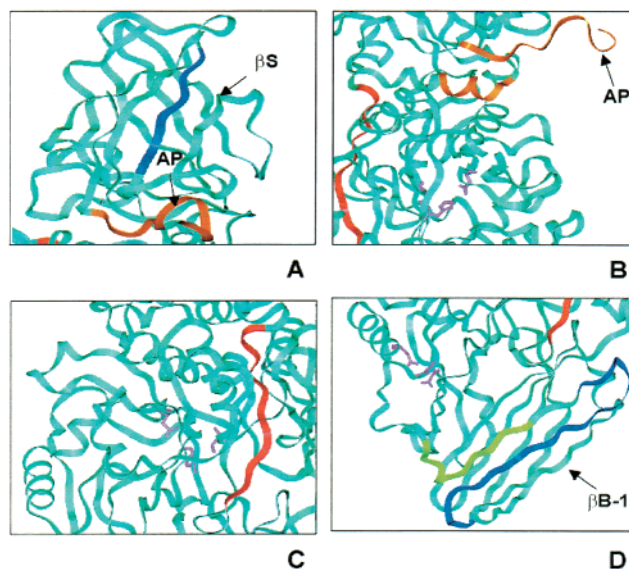


FIGURE 5: Illustration of observed changes in solvent accessibility in the context of the 1FIE X-ray crystal structure of the FXIII  $\alpha$ -subunit. The colors used in this figure represent the degree of deuteration upon activation and whether it is increasing or decreasing. Increases are depicted in orange (less than 4.5%) and red (greater than 4.5%). Decreases are depicted in green (less than 4.5%) and blue (greater than 4.5%). Panel A: the activation peptide and  $\beta$ -sandwich domain. Panel B: the activation peptide and catalytic core domain displayed from the “front” (the orientation depicted in Figure 1), to demonstrate the proximity of the activation peptide and the short helix spanning residues 240–247. The active site residues are depicted as pink sticks (here and in Panel C). Panel C: the domains displayed in Panel B are rotated 180° (the “back” of the enzyme, relative to Figure 1). Note the segment spanning residues 220–230 (part of the peptide 7 region) and its proximity to the active site residues. Panel D: the  $\beta$ -barrel 1 domain. A small portion of the catalytic core is visible in this view. The pink sticks here represent the residues of the putative calcium binding site in the enzyme.

The magnitude of this change is reduced to half when the enzyme is in the  $a_2^*$  state. There is almost no change in percent deuteration in this segment for the  $a_2'$  state of the enzyme.

There is also a portion of the  $\beta$ -sandwich domain, residues 98–104, that shows a large decrease in percent deuteration in the  $a_2^{*Ca}$  state (Figure 5A). The decrease of 0.55 Da in the centroid of this mass envelope equates to a 8.37% decrease in deuteration. The discovery that another peptide, 1508.7861  $m/z$ , residues 100–111, overlapping part of this

particular peptide shows no change in percent deuteration at all upon exposure to calcium leads to the conclusion that this effect is localized to the residues 98 and 99. It was not possible to observe the behavior of this region of the protein in the  $a_2^*$  or  $a_2'$  state of the enzyme, as this peak is not observed in the peptic digest of the thrombin-cleaved enzyme.

A portion of the catalytic core of the enzyme spanning residues 220–230 becomes slightly more deuterated upon activation (Figure 5C). The magnitude of the increase ( $\sim 4.5\%$ ) is almost equivalent for both the  $a_2^*$  and  $a_2^{*Ca}$  states of the enzyme. There is a decrease in the degree of deuteration of this region, from 4.5% to 2.9%, when the enzyme goes from the  $a_2$  to the  $a_2'$  state, hinting at a distinct role for calcium in this activation event.

Another portion of the catalytic core is represented by the peptide spanning residues 240–247. This is a short helical region of the core that is very close to the activation peptide segment, as shown in Figure 5B. This helix exhibits an approximately 5% increase in solvent accessibility which cannot be reliably quantified, due to the presence of a peak cluster that overlaps with this mass envelope upon deuteration. The behavior of the centroid, however, when referenced to the zymogen state of the enzyme allows us to classify this region of the core as increasing in percent deuteration in all of the activation events investigated.

Other portions of the protein are experiencing even smaller changes in percent deuteration upon activation. These areas include the activation peptide itself, which appears to become slightly more deuterated in all of the activation events studied (Figure 5A,B). When the enzyme is activated solely by exposure to high levels of calcium, the degree of deuteration is slightly less.

In the  $\beta$ -barrel 1 domain, residues 513–522 experience a small decrease in deuteration, shown in Figure 5D. These residues are a part of a linker between the  $\beta$ -barrel 1 and the catalytic core. The effect may be sensitive to the presence of calcium, as the enzyme in the  $a_2'$  state, with no additional calcium in the buffer, appears to be slightly lower. This result correlates with the previously observed larger decrease in percent deuteration in residues 526–546.

## DISCUSSION

This study addresses from a structural standpoint the observed differences between FXIII activated proteolytically by thrombin cleavage and nonproteolytically by exposure to high levels of calcium. The results seek to provide further insight into the separate roles of thrombin and calcium in bringing the enzyme to full activity.

**Sequence Coverage by Enzymatic Digests.** Both peptic and tryptic digests of the protein result in a moderate degree of sequence coverage, although fragments from several structurally important regions of FXIII were observed in a typical enzymatic digest. Several of the peaks observed also occur as overlapping clusters, and it is possible that missing sequence coverage may be associated with some of these overlapped mass envelopes. Other fragments representing further sequence coverage may also be generated, but may not be susceptible to ionization in the MALDI-TOF MS.

X-ray crystallographers have previously concluded that neither activation of the enzyme by thrombin nor exposure

to calcium are sufficient to initiate the large-scale conformational change that is believed to be necessary to expose the catalytic triad of FXIII (16). Indeed, in the current isotope exchange/mass spectrometry studies, no peptic fragments have yet been isolated that contain residues of the catalytic triad, Cys 314, His 373, and Asp 396. The catalytic core's resistance to proteolysis makes it likely that even in solution, activation of the enzyme by cleavage with thrombin or exposure to calcium does little to expose this portion of the protein to the bulk solvent environment.

**Effects of Thrombin Cleavage and Calcium Binding on the Activation Peptide.** Changes in percent deuteration observed range from 2.5% to 8.37% in the current study. There is precedence for accepting changes of 5–10% as significant (25, 31). The emphasis here will be placed on percent deuteration changes of 4.5% or higher.

The observation that rFXIII can assume the same level of activity when incubated in the presence of 50mM calcium chloride as it does when cleaved by thrombin in the presence of much lower levels of calcium (8, 9) forms much of the basis of this study. Although rFXIII  $a_2^{*Ca}$  loses its activity when it is exchanged into a calcium-free buffer, the addition of calcium can restore the enzyme to full activity. In either activation scenario, the active site must become exposed somehow, possibly through movement of the activation peptide or other domains of the enzyme. This leads one to wonder if thrombin cleavage and calcium binding result in similar structural changes in platelet FXIII, or if each event results in activation of the enzyme by a different pathway.

X-ray crystallography has shown that the activation peptide remains noncovalently associated with the enzyme, even after being cleaved by thrombin (14). This has since been verified through mass spectrometry. Activation of FXIII by thrombin cleavage followed by ultrafiltration through a membrane having a molecular weight cutoff of 50 kDa is expected to result in the loss of the  $\sim 4000$  Da segment. However, MALDI-TOF mass spectra on samples prepared in this manner clearly show the presence of a peak at 79 kDa (corresponding to thrombin-cleaved FXIII) and a second peak at 3910 Da (data not shown). These results agree substantially with previous studies of the thrombin-cleaved enzyme performed by electrospray mass spectrometry (32).

The activation peptide segment spanning positions 4–20 (Figure 5A, in orange) experiences a small increase in percent deuteration following activation of the enzyme that seems to be at its highest in the  $a_2^*$  state. This does not differ substantially, however, from the change that is observed for  $a_2^{*Ca}$ . The results therefore agree with previous results reported from X-ray crystallography, which predicts no significant movement of the activation peptide upon activation. It is possible that such a large-scale conformational change in this region or the departure of the activation peptide will not occur until substrates are introduced.

**Increased Deuteration of a Possible Substrate Recognition Site in the Catalytic Core.** A region of the catalytic core spanning residues 220–230 becomes up to 4.55% more deuterated upon activation of the enzyme. This increase in deuteration occurs to a greater degree in the presence of calcium, as evidenced by the lower degree of deuteration observed when the enzyme is thrombin-cleaved and deprived of calcium. (Figure 5C, in red) A fragment of FXIII termed "peptide 7" spans residues 190–230 and has been reported



to be an inhibitor of FXIII (33). It was shown to compete with the enzyme for the binding of glutamine-containing substrates, and thus peptide 7 was believed to be a possible substrate recognition region in the enzyme. Attempts to localize the binding area of peptide 7 comprised of manufacturing synthetic peptides representing various regions of peptide 7. Although the inhibitory properties of whole peptide 7 were demonstrated to be much greater than the sum of those of its individual parts, one portion, spanning residues 221–230, exhibited modest inhibition of fibrin cross-linking and the incorporation of artificial peptide substrates into lysine-containing donors by FXIII.

The increased degree of deuteration of residues 220–230 upon activation may provide an insight into the mechanism of FXIII. It may result from increased exposure of this possible substrate recognition region to the bulk solvent as a necessary first step in preparing the enzyme for binding glutamine-containing substrates. This is known to be the first substrate that binds to the enzyme according to the ping-pong mechanism (reviewed in 4).

A portion of the catalytic core spanning residues 240–247 exhibits an increase in deuteration in the  $a_2^*$  state. The degree of the change cannot be accurately quantified due to the fact that a second peak cluster (monoisotopic  $m/z = 1011.4549$ ) overlaps with this peak cluster. A qualitative analysis of this overlapped mass envelope allows us to conclude that this small, helical portion of the protein exhibits a slight increase in degree of deuteration upon activation and in the presence of calcium. The proximity of this helix to the activation peptide segment in rFXIII is intriguing. (Figure 5B, in orange).

*Changes in the  $\beta$ -Sandwich Domain: A Long-Range Effect of Calcium Binding?* The most interesting observation within the  $\beta$ -sandwich domain is a peptide spanning residues 98–104 of the protein (Figure 5A, in blue). It shows a decrease in percent deuteration of 8.37% in the  $a_2^{*Ca}$  state. This particular peptide is not observed at all in the mass spectra of digests of either  $a_2'$  or  $a_2^*$ . It was first believed that this might be a portion of the activation peptide, which is cleaved by thrombin. However, the identity of this peptide by post-source decay analysis precludes this possibility. Furthermore, MALDI-TOF mass spectrometry on the whole thrombin-cleaved enzyme as described above shows that the activation peptide is still present even after being cleaved by thrombin. A peptide segment (100–111) that has been identified as overlapping the 98–104 peptide shows no change in degree of deuteration at all under the same conditions, leading us to the conclusion that the change is localized to the residues Leu 98 and Phe 99.

Residues 98–104 are quite distant from the proposed calcium binding site in the enzyme. It is not known why this particular peptide cannot be observed in the mass spectra of pepsin digests derived from thrombin-cleaved rFXIII. It is possible that this portion of the protein becomes inaccessible to peptic cleavage after the enzyme is activated by thrombin. Ionization of this peptide may be suppressed by an unknown mechanism following thrombin activation as well. The role of a conformational change in this region is similarly unclear, but may be linked to calcium binding.

*$\beta$ -Barrel 1 Domain: Decreased Deuteration.* The decrease in percent deuteration of the  $\beta$ -barrel 1 domain peptide spanning residues 526–546 (Figure 5D, in blue) is 6.83%

upon exposure of the zymogen to 50mM calcium to produce  $a_2^{*Ca}$ . The thrombin-cleaved enzyme  $a_2'$  shows no change at all compared to the zymogen  $a_2$ , whereas the  $a_2^*$  form shows a smaller decrease in percent deuteration with respect to the zymogen. A more minor change is observed in the same protein domain, in a peptide spanning residues 513–522 (Figure 5D, in green), that also exhibits the same dependence on calcium. The magnitude of the change in 526–546 points to a dependence on calcium; the change is greatest when the enzyme is activated only by exposure to calcium and is reduced to half when thrombin is used to cleave the enzyme and a low level of calcium is left in the buffer. The effect disappears almost completely when the enzyme is cleaved by thrombin and then exchanged into a calcium-free buffer. It appears to support the view of calcium as an allosteric effector, as proposed by Hornyak and Shafer (7).

The fact that the changes observed are subtle is in line with the observation that X-ray crystal structures of the enzyme in each of these states are not fundamentally different from one another. Previous studies have reported increased exposure of the active site thiol group (Cys 314) upon cleavage of the activation peptide and/or exposure to calcium based on the rate of incorporation of  $^{14}C$ -iodoacetamide (7, 13). Yet X-ray crystallography fails to show any sign of a large-scale conformational change in the enzyme upon either of these activation events (14, 16, 17). The apparent conflict may be resolved by noting that iodoacetamide is substantially smaller than other macromolecular substrates processed by Factor XIII. Therefore, the more subtle conformational changes suggested by our observations may be sufficient to permit access of small molecule substrates to the active site while being undetectable by X-ray crystallography.

*Placing the Results in the Context of the Total Model.* A number of conclusions can be drawn regarding the mechanism of FXIII activation on the basis of the H/D exchange results. The activation peptide remains associated with the enzyme, even after proteolytic cleavage by thrombin. It experiences a modest increase in percent deuteration which may be best characterized as relatively insensitive to the method of activation.

Increased deuteration of the peptide 7 region might be correlated with increased exposure of this region to the bulk solvent, possibly in preparation for binding a glutamine-containing substrate. The decreased deuteration observed in the  $\beta$ -barrel 1 domain may be related to a previously proposed mechanism in which the  $\beta$ -barrel 1 domain must roll away from the catalytic core (14) to permit greater access to the active site. These changes in percent deuteration may intensify upon introduction of a substrate. Earlier studies have suggested a conformational change in Factor XIII triggered by the glutamine-containing substrate (34).

In all cases, the presence of calcium appears to intensify the observed changes in percent deuteration. Activation by exposure of the enzyme to high levels of calcium appears to mimic the effects observed in activation catalyzed by thrombin cleavage. This strongly suggests a role for calcium as an allosteric effector. The effects of calcium binding can be local, as observed in the  $\beta$ -barrel 1 domain's decrease in percent deuteration, but can also be truly long-range, as evidenced by its impact on the  $\beta$ -sandwich domain. The decrease in percent deuteration observed in residues 98–104, relatively distant from the calcium binding site, is unique

and will certainly warrant further study to elucidate its cause and function.

In summary, our results complement findings from X-ray crystallography and kinetics by presenting a view of protein dynamics under solution conditions. Future work will focus on measuring changes in the percent deuteration of FXIII upon binding to both natural and artificial peptide substrates and in the presence of a fibrin surface.

## ACKNOWLEDGMENT

We thank Dr. Paul Bishop of ZymoGenetics, Inc., Seattle, WA, for the gift of recombinant placental Factor XIII a<sub>2</sub>. This project has benefited greatly from initial training provided by Prof. Elizabeth A. Komives, UCSD, during her time as a University of Louisville Brown & Williamson Scholar, September 2000. We further appreciate receiving a copy of the CAPP program developed in her laboratory. Our thanks also to D.B. Cleary, G. Isetti, and T.A. Trumbo for helpful conversations during the course of this research.

## REFERENCES

- Halkier, T. (1991) *Mechanisms in Blood Coagulation, Fibrinolysis and the Complement System*, Cambridge University Press, Cambridge.
- Sakata, Y., and Aoki, N. (1982) *J. Clin. Invest.* 69, 536–542.
- Bishop, P. D., Teller, D. C., Smith, R. A., Lasser, G. W., Gilbert, T., and Seale, R. L. (1990) *Biochemistry* 29, 1861–1869.
- Muszbek, L., Yee, V. C., and Hevessy, Z. (1999) *Thromb. Res.* 94, 271–305.
- Pedersen, L. C., Yee, V. C., Bishop, P. D., Le Trong, I., Teller, D. C., and Stenkamp, R. E. (1994) *Protein Sci.* 3, 1131–1135.
- Yee, V. C., Pedersen, L. C., LeTrong, I., Bishop, P. D., Stenkamp, R. E., and Teller, D. C. (1994) *Proc. Natl. Acad. Sci. U.S.A.* 91, 7296–7300.
- Hornyak, T. J., and Shafer, J. A. (1991) *Biochemistry* 30, 6175–6182.
- Polgár, J., Hidasi, V., and Muszbek, L. (1990) *Biochem. J.* 267, 557–560.
- Credo, R. B., Curtis, C. G., and Lorand, L. (1978) *Proc. Natl. Acad. Sci. U.S.A.* 75, 4234–4237.
- Lewis, S. D., Janus, T. J., Lorand, L., and Shafer, J. A. (1985) *Biochemistry* 24, 6772–6777.
- Naski, M. C., Lorand, L., and Shafer, J. A. (1991) *Biochemistry* 30, 934–941.
- Hornyak, T. J., and Shafer, J. A. (1992) *Biochemistry* 31, 423–429.
- Hornyak, T. J., Bishop, P. D., and Shafer, J. A. (1989) *Biochemistry* 28, 7326–7332.
- Yee, V. C., Pedersen, L. C., Bishop, P. D., Stenkamp, R. E., and Teller, D. C. (1995) *Thromb. Res.* 78, 389–397.
- Weiss, M. S., Metzner, H. J., and Hilgenfeld, R. (1998) *FEBS Lett.* 423, 291–296.
- Yee, V. C., Le Trong, I., Bishop, P. D., Pedersen, L. C., Stenkamp, R. E., and Teller, D. C. (1996) *Semin. Thromb. Hemostasis* 22, 377–384.
- Fox, B. A., Yee, V. C., Pedersen, L. C., Le Trong, I., Bishop, P. D., Stenkamp, R. E., and Teller, D. C. (1999) *J. Biol. Chem.* 274, 4917–4923.
- Zhang, Z., and Smith, D. L. (1993) *Protein Sci.* 2, 522–531.
- Mandell, J. G., Falick, A. M., and Komives, E. A. (1998) *Anal. Chem.* 70, 3987–3995.
- Hughes, C. A., Mandell, J. G., Anand, G. S., Stock, A. M., and Komives, E. A. (2001) *J. Mol. Biol.* 307, 967–976.
- Andersen, M. D., Shaffer, J., Jennings, P. A., and Adams, J. A. (2001) *J. Biol. Chem.* 276, 14204–14211.
- Resing, K. A., and Ahn, N. G. (1998) *Biochem.* 37, 463–475.
- Engen, J. R., Gmeiner, W. H., Smithgall, T. E., and Smith, D. L. (1999) *Biochemistry* 38, 8926–8935.
- Tuma, R., Coward, L. U., Kirk, M. C., Barnes, S., and Prevelige, P. E., Jr. (2001) *J. Mol. Biol.* 306, 389–396.
- Wang, L., Lane, L. C., and Smith, D. L. (2001) *Protein Sci.* 10, 1234–1243.
- Trumbo, T. A., and Maurer, M. C. (2000) *J. Biol. Chem.* 275, 20627–20631.
- Fickenscher, K., Aab, A., and Stüber, W. (1991) *Thromb. Haemostasis* 65, 535–540.
- Patterson, D. H., Tarr, G. E., Regnier, F. E., and Martin, S. A. (1995) *Anal. Chem.* 67, 3971–3978.
- Rosa, J. J., and Richards, F. M. (1979) *J. Mol. Biol.* 133, 399–416.
- Englander, J. J., Rogero, J. R., and Englander, S. W. (1985) *Anal. Biochem.* 92, 517–524.
- Chen, J., and Smith, D. L. (2001) *Protein Sci.* 10, 1079–1083.
- Ashcroft, A. E., Grant, P. J., and Ariens, R. A. (2000) *Rapid Commun. Mass Spectrom.* 14, 1607–1611.
- Achyuthan, K. E., Slaughter, T. F., Santiago, M. A., Enghild, J. J., and Greenberg, C. S. (1993) *J. Biol. Chem.* 268, 21284–21292.
- Mitkevich, O. V., Shainoff, J. R., DiBello, P. M., Yee, V. C., Teller, D. C., Smejkal, G. B., Bishop, P. D., Kolotushkina, I. S., Fickenscher, K., and Samokhin, G. P. (1998) *J. Biol. Chem.* 273, 14387–14391.

BI025630N